Green Energy and Resources 1 (2023) 100031

Contents lists available at ScienceDirect

Green Energy and Resources

journal homepage: www.journals.elsevier.com/green-energy-and-resources

Recent advances in single-atom catalysts for electrocatalytic synthesis of hydrogen peroxide

Helai Huang [a,1], Mingze Sun [a,1], Mei Li [b,**], Lei Tang [c,***], Shengbo Zhang [a,*]

[a] State Key Laboratory of Chemical Engineering, Department of Chemical Engineering, Tsinghua University, Beijing 100084, China
[b] Key Laboratory for Green Chemical Technology of the Ministry of Education, School of Chemical Engineering and Technology, Collaborative Innovation Center of Chemical Science and Engineering, Tianjin University, Tianjin 300072, China
[c] Department of Chemical and Biomolecular Engineering, National University of Singapore, 4 Engineering Drive 4, Singapore 117585, Singapore

ARTICLE INFO

Keywords:
Hydrogen peroxide
Electro-synthesis
Single-atom catalysts
Structure regulation
Activity and selectivity

ABSTRACT

The electro-synthesis of hydrogen peroxide has attracted extensive research interest and is expected to replace conventional chemical processes as a mild and safe approach. Single-atom catalysts (SACs) have been applied in a wide variety of thermo- and electro-chemical reactions due to their high atom utilization and highly tunable electronic structure. Herein, an in-depth discussion on recent advances of SACs in the field of hydrogen peroxide electro-synthesis is summarized, specifically on the surface structure and electronic effects that enable high activity and selectivity of SACs. Different synthesis and modification strategies of SACs are discussed in detail, emphasizing the remarkable versatility of SACs utilization in this field. Finally, the opportunities and challenges of SACs for electrocatalytic synthesis of hydrogen peroxide are summarized in terms of rational design, controlled synthesis, and the stability of operation at high current densities of SACs to meet practical requirements.

1. Introduction

Hydrogen peroxide is an extensively used chemical both for public and household purpose, which lead to an overall production over 5.5 million tons per year (Ciriminna et al., 2016; Jiang et al., 2020). It could work as a medical disinfectant (Caruso et al., 2020; Flores et al., 2012; Jatta et al., 2021), an important raw material in chemical synthesis (Noyori et al., 2003; Lane and Burgess, 2003), and more importantly, a green oxidant in many fields (Hage and Lienke, 2005; Zhang et al., 2020a; Yang et al., 2018) (Fig. 1(a)). H_2O_2 is not only a green oxidant itself, many technologies use hydrogen peroxide as a precursor reagent to produce hydroxyl radicals (·OH), and this process of using radicals for organic oxidation and contaminant removal is called Advanced Oxidation Process (AOP). These techniques include the incorporation of iron salts or heterogeneous Fenton catalysts to accelerate the radical generation process (Liu et al., 2023a; Zhou et al., 2022), integration with electrochemical and photochemical processes to facilitate the Fenton cycle (Brillas et al., 2009, 2019), combination with other oxides such as ozone and persulfates (Kodavatiganti et al., 2021), or coupled with UV or ultrasound techniques (Barazesh et al., 2015). These techniques have been extensively used in the field of wastewater treatment (Kosaka et al., 2001; Chidambara Raj and Li Quen, 2005). Nowadays, industrial synthesis of H_2O_2 is mostly through an anthraquinone process, this method involves hydrogenation and oxidation of anthraquinone on Pd-based catalyst (Santacesaria et al., 1999, 2002). Despite the low energy cost and high degree of automation of this method, anthraquinone process produces highly concentrated (30%~70%) hydrogen peroxide solution in a centralized form, which possesses risk in storage and transportation (Jiang et al., 2018; Yamanaka and Murayama, 2008), especially for citizens living in central and western China. Besides, few applications, except for aerospace industry and special-purpose industrial synthesis, required H_2O_2 in this highly-concentrated form. What's more, anthraquinone is difficult to recycle efficiently and various degradation products are produced in this process (Kosydar et al., 2010). As a result, anthraquinone has to be successively replenished to enable continuously production, which could not meet the requirements of green chemistry (Campos-Martin et al., 2006). Therefore, a decentralized method to produced low concentration hydrogen peroxide solution is highly desirable.

* Corresponding author.
** Corresponding author.
*** Corresponding author.
E-mail addresses: li1528619076@163.com (M. Li), lei01@nus.edu.sg (L. Tang), zhangshengbo@tsinghua.edu.cn (S. Zhang).
[1] These authors contributed equally: Helai Huang, Mingze Sun.

https://doi.org/10.1016/j.gerr.2023.100031
Received 9 April 2023; Received in revised form 6 June 2023; Accepted 10 July 2023

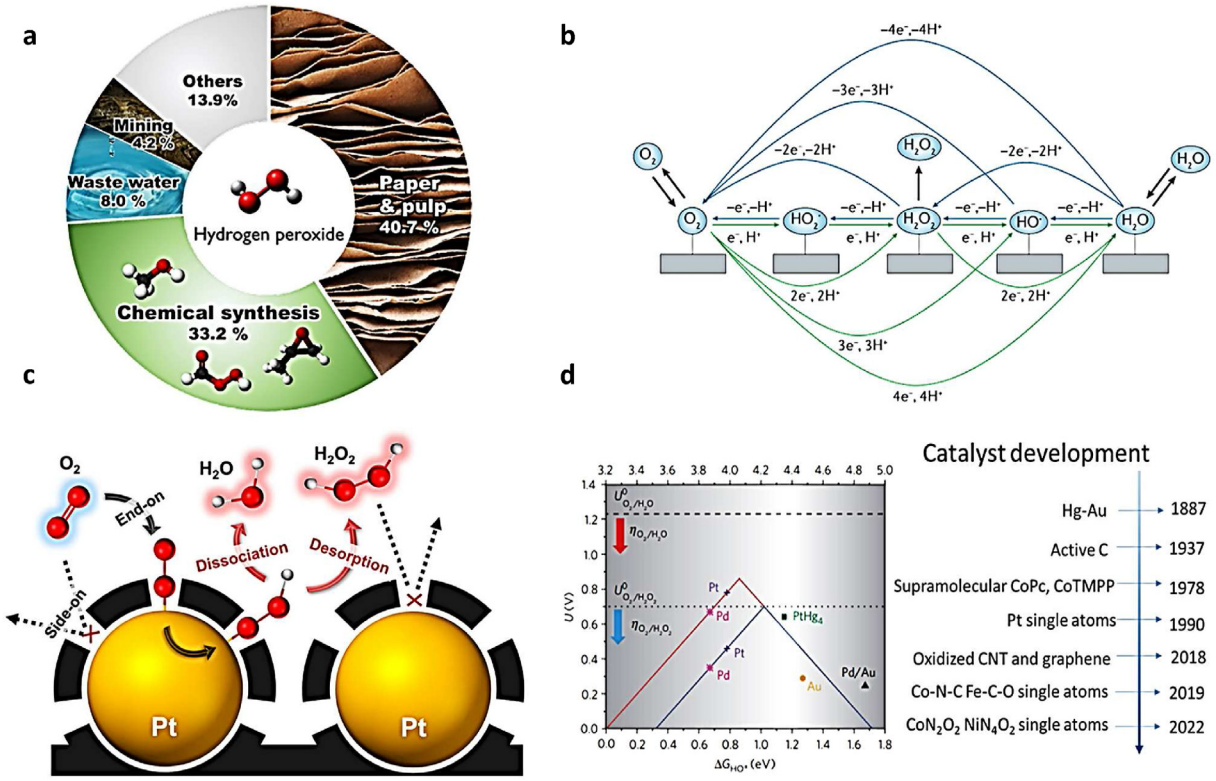

Fig. 1. (a) The hydrogen peroxide market share in the USA in 2015 (Yang et al., 2018). (b) The possible reduction pathways and oxidation pathways of O_2-related reactions, stoichiometric H_2O omitted for clarity (Perry et al., 2019). (c) End-on configuration on a carbon-coated Pt catalyst and the competing dissociation and desorption pathways, the existence of carbon hinders further reduction of H_2O_2 (Choi et al., 2014). (d) Catalyst development path of electro-catalysts through two electron ORR, reproduced and modified from references (Zhang et al., 2020b; Siahrostami et al., 2013).

Electrochemical synthesis method produces a new route for on-site production of hydrogen peroxide. The energy sources could come from renewable energy and the only by-product is water. What's more inspiring, the reaction could be performed at mild working conditions and the production rate could be controlled by simply changing the applied voltage. H_2O_2 could be produced either from O_2 or H_2O, however, the anodic oxidation of H_2O to H_2O_2 is far from satisfactory and lack sufficient catalysts (Shi et al., 2017; Fuku et al., 2017). As a result, researchers are dedicated to design catalysts and reactor configurations to produce H_2O_2 through two electron oxygen reduction reaction (ORR). Nevertheless, a number of obstacles should be addressed: (1) Most catalysts prefer four electron ORR, but the selectivity and stability of most catalysts are far from satisfactory (Gao and Liu, 2020). (2) H_2O_2 is very likely to decompose or go through a further reduction to form H_2O, which brings a lot of risks in mass transfer and reactor design. (3) Most reactor configurations today have low efficiency and productivity (Zhang et al., 2020b).

Single-atom catalysts have emerged as a new class of heterogeneous catalysts over the past decade (Su et al., 2020; Cui et al., 2018; Qiao et al., 2011; Li et al., 2020a), and have been extensively studied due to their distinct metal-substrate interactions and full utilization of metal atoms. Due to this special dispersity, SACs have a wide application both in thermo- (Kaiser et al., 2020; Ro et al., 2022; Liu et al., 2017; Wang et al., 2016) and electro- (Chung et al., 2017; Zhang et al., 2018; Jung et al., 2020; Chen et al., 2021a, 2022a; Sun et al., 2022) chemical reactions, and have been confirmed to either enhance the activity and selectivity of reactions or to explore the reaction mechanisms (Zhang et al., 2021, 2023). While most pure metal nanoparticles (except Hg) would only generate limited amount of H_2O_2 at low overpotentials (Perry et al., 2019), both noble metal SACs, Pt, Pd, and non-noble metal SACs, including Fe, Co, Ni, Mo, etc., have shown promising activity in laboratory scale H_2O_2 production. Due to this unusual activity towards two electron ORR, these SACs have received tremendous research interest (Choi et al., 2016; Song et al., 2020; Tian et al., 2022). Researchers have also studied the impact of local coordination environments on the catalytic performance (Zhu et al., 2019; Qin et al., 2020; Zhao et al., 2020), including macroscopic substrate modulation, first sphere modification by directly changing the coordination atoms, and second sphere modification by introducing functional groups. Current synthesis method often includes combining C, N and metal sources either in a single compound or included separately in different precursors. The compounds are commonly pyrolysis in furnace in a temperature range of 700~1100°C. During the pyrolysis process, the single metal atoms diffused into the nitrogen doped carbon matrix and formed the MN_X motifs at high temperature above 600°C. This is called the vapor-phase single atom transport mechanism (Li et al., 2019a). The synthesis mechanism relies strongly on the choice of metal precursor, metal content, pyrolysis temperature and synthesis procedures. As a consequence, it is still difficult to elucidate the exact anchoring processes of different SACs, and detailed structures of MN_X architectures and their physico-chemical properties is also under debate. However, these synthetic efforts greatly enriched single-atom catalysts family and provided us with more opportunities to obtain high performance catalysts, and will be further discussed in this review.

These advantages of SACs may arise from the thermodynamics of oxygen-related reactions (Fig. 1(b)). The competing two electron (R1) and four electron (R2) reaction hinders the development of catalysts. The reactivity and selectivity strongly related with *OOH intermediates on the catalyst surface. If the catalysts bind *OOH intermediates too strongly, it will not go through the protonation process to form H_2O_2 (R3), but will go through the dissociation process to form H_2O (R4).

2 electron ORR pathway $O_2 + 2H^+ + 2e^- \rightarrow H_2O_2$ (R1)

4 electron ORR pathway $O_2 + 4H^+ + 4e^- \rightarrow 2H_2O$ (R2)

*OOH protonation $*OOH + H^+ + e^- = H_2O_2 + *$ (R3)

*OOH dissociation $*OOH + H^+ + e^- = H_2O + *O$ (R4)

The binding energy of these intermediates plays a vital role in catalyst design, and could be carefully controlled by modification of the catalyst surface and electronic structure. According to Choi's observation (Kosydar et al., 2010) (Fig. 1(c)), on the bulk Pt/C surface, the oxygen molecule tends to favor "side-on" binding configuration, that is, two oxygen atoms bind on adjacent Pt atoms. Through this configuration, the O–O bond is weakened and thus easy to break to undergo a four electron ORR pathway. However, through a subsequent controlled coating of amorphous carbon onto the Pt/C surface, Pt atoms are isolated and oxygen could only form an "end-on" binding mood, which greatly enhanced two electron ORR. Researchers also confirm the existence of isolated Pt and Pd atoms on PtHg (Siahrostami et al., 2013) and PdAu (Jirkovsky et al., 2011) alloys strongly favoring H_2O_2 production. These experiments strongly supported the role of isolated atoms on the activity of catalysts, and provides a more theoretical basis for the development of single-atom catalysts.

Aside from the traditional synthesis of hydrogen peroxide under alkaline conditions, Pt and Co SACs also tends to perform very well in acid electrolytes (Shen et al., 2019; Chen et al., 2022b), far exceeding carbon-based material counterparts. Synthesis of hydrogen peroxide under acidic conditions has certain advantages, such as hydrogen peroxide is more stable under acidic conditions, because OH^- itself can catalyze the decomposition of hydrogen peroxide (Qiang et al., 2002). Secondly, the hydroxide fuel cell has many problems such as poor membrane stability, low mass transfer efficiency and low activity of hydrogen oxidation reaction (Ayers et al., 2012; Sheng et al., 2010). Meanwhile, the electro-fenton process under acidic conditions could be applied in the field of water treatment (Xu et al., 2021). As a result, developing more SACs working in acid electrolyte is also pursuable. The development path of electro-catalysts is summarized here (Fig. 1(d)).

In this review, we will take a step forward to the rational catalyst design of recently reported SACs. Both noble-metal SACs and non-noble metal SACs will be discussed in depth, with an emphasis on versatile synthesis and modification methods. SACs working in acid electrolyte and at high working current densities will be further highlighted and proposed.

2. Noble metal SACs

Platinum-group metals (PGM) are the state-of-the-art catalysts for 4-electron oxygen reduction reaction (ORR) in fuel cell technologies (Stamenkovic et al., 2007; Gong et al., 2023). However, when the active sites change to be atomically dispersed, ORR has been proved to squint towards a 2-electron pathway that predominantly generates H_2O_2 (Perry et al., 2019; Choi et al., 2016). For example, Kim et al. prepared a sort of atomically dispersed precious metal catalysts which all exhibited higher H_2O_2 selectivity than their counterpart nanoparticles (Fig. 2(a)) (Kim et al., 2020). The enhanced H_2O_2 selectivity may because the isolated sites favor end-on (Pauling-type) adsorption of O_2 rather than side-on adsorption as previously discussed.

Single-atom platinum catalysts have been widely investigated in electrocatalytic synthesis of hydrogen peroxide. To the beginning, Pt sites was separated by electrodepositing Hg on Pt nanoparticles and then an ordered intermetallic structure was formed with isolated Pt atoms surrounded by Hg (Fig. 2(b)). (Siahrostami et al., 2013) This rational design boosted the activity and showed high selectivity above 90% for H_2O_2 production. Recently, inspired by the development of single-atom catalysts, platinum SACs supported on different substrates have been successfully synthesized. For example, Choi et al. designed an atomically dispersed Pt catalyst embedded in sulfur-doped zeolite-templated carbon via a mild wet-impregnation method. With large sulfur content (17 wt% S) and a unique carbon structure, this catalyst stabilizes a high-loading of Pt (5 wt%) and thus high H_2O_2 selectivity (Fig. 2(c)) (Choi et al., 2016). To further increase the metal loading, single atomic Pt supported on hollow CuS_x was designed to meet the requirement of high concentration Pt sites (Fig. 2(d)) (Shen et al., 2019). With 24.8 at% Pt loading, the obtained sample showed high activity and selectivity for O_2 reduction to H_2O_2 over a wide potential range. This precisely illustrates that increasing the metal loading to improve catalytic activity is of great significance. Furthermore, the choice of substrates can also affect the ORR selectivity on Pt SACs. The support effect in Pt SACs was studied by comparing Pt_1/TiC and Pt_1/TiN (Fig. 2(e)) (Yang et al., 2017). At 0.1 V vs RHE, the selectivity of the former is 75% while only 47% remains on the latter. The DFT analysis revealed that the dissociation of O_2* to 2O* or

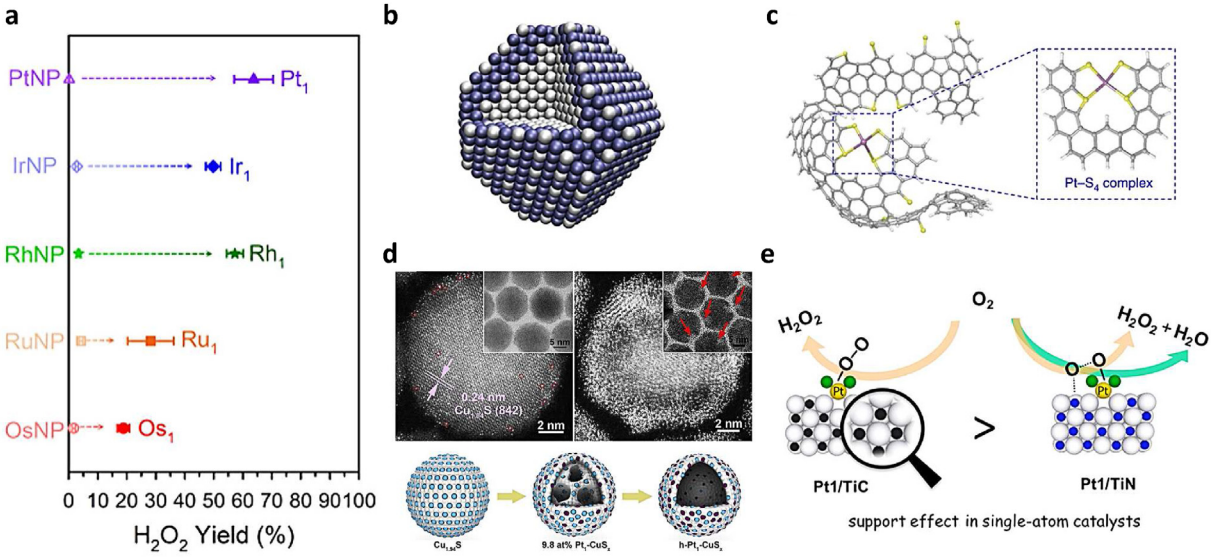

Fig. 2. (a) H_2O_2 yields of different PGM-SAC catalysts as well as their nanoparticles counterparts at −0.5 mA cm^{-2} (Kim et al., 2020). (b) Schematic representation of isolation Pt sites on a Pt–Hg/C nanoparticle (Siahrostami et al., 2013). (c) Schematic representation of Pt SAC on sulfur-doped zeolite-templated carbon (Choi et al., 2016). (d) TEM images and schematic representation of single atomic Pt supported on hollow CuS_x (Shen et al., 2019). (e) Schematic representation of the support effect in Pt SACs with high H_2O_2 selectivity for Pt_1/TiC than Pt_1/TiN (Yang et al., 2017).

OOH* to O* + OH* has an activation barrier of 0.19 eV or 0.51 eV on Pt_1/TiC while barrier-free on Pt_1/TiN. These barrier-free steps provide stronger affinity of oxygen species thus poisoning the catalyst surface. This emphasizes the important role of substrate selection to tune the ORR pathway. In summary, the coordination structures and the supports of Pt SAC can be cleverly adopted to boost the activity and selectivity of H_2O_2 electro-synthesis.

Besides platinum, other platinum-group metals such as palladium and rhodium also show great potential on e-H_2O_2 synthesis. Ledendecker et al. reported the synthesis of atomically dispersed $PdCl_x$/C for H_2O_2 production (Ledendecker et al., 2020). The $PdCl_x$/C SAC achieved a H_2O_2 selectivity of above 90% with a mass-normalized activity of 72.8 A g_{Pd}^{-1}, together with a great stability even after 1000 degradation cycles (Fig. 3(a)). Kim et al. also prepared Pd single-atom catalyst on C@C_3N_4 support, and compared Pd with Pt single atoms for H_2O_2 production (Kim et al., 2019). The C@C_3N_4-0.5 %Pd catalyst showed higher selectivity up to 94% than C@C_3N_4-0.5 %Pt under 60%. DFT calculations evidenced that O–O bond length was shorter on Pd single atom than on Pt atom (1.34 Å versus 1.31 Å), thus having a lower O_2 binding energy and preventing H_2O formation. Cao et al. systematically studied up to 25 SACs including Ir, Os, Pd, Au supported on g-C_3N_4 by *ab initio* molecular dynamics simulations method as well as DFT calculations (Fig. 3(b)) (Cao et al., 2020). They found that the N-vacancy g-C_3N_4 doped with Pd–Cu hybrid double atoms (PdCu @ V_C_3N_4) impended over the top of the two-electron volcano plot. This suggests that alloying SAC or designing DAC may be an effective strategy for selective H_2O_2 production. Rh SACs are also promising catalysts for H_2O_2 production (Kim et al., 2020; Chen et al., 2022c). Chen et al. designed an enzyme-like Rh SAC to simulate the properties of flavoenzymes for the H_2O_2 production under mild conditions (Fig. 3(c)). This novel structure can achieve the 100% selectivity of H_2O_2 production and can be widely-applied in different substrates.

In summary, due to the excellent activity of precious metals for oxygen reduction reactions, PGM catalysts are the well-known and most widely used electrocatalysts for ORR. When the metal sites are atomically distributed on the substrate, the ORR reaction on catalysts will change from 4-electron pathway to a 2-electron pathway (Jiang et al., 2018). The high activity and selectivity can be achieved by exquisitely tuning the coordinate structure as well as the metal-support interactions (MSI). However, due to the low abundance of PGMs in the earth, the price of PGMs is relatively high, which leads to an inevitable increase of the cost. Based on this consideration, non-PGM SACs have been extensively studied in recent years.

3. None-noble metal SACs

None-noble metal SACs have been worked as an alternative of PGM based catalyst in a wide range of electro-catalytic reactions, especially as a cathodic catalyst in Proton Exchange Membrane Fuel Cell (PEMFC). While the most studied M-N-C configuration have meet expectations in $4e^-$ ORR and their activity in PEMFC have surpassed commercial Pt/C catalyst, few studies have focused on their activity towards $2e^-$ ORR. Take the traditional CoN_4 SAC as an example, prior reports indicate that CoN_4 is a promising material in fuel cell applications for its relatively sluggish fenton process with high stability (He et al., 2019; Wang et al., 2018). The Co–N–C catalyst (Xie et al., 2020) could achieve a high half wave potential ($E_{1/2}$) of 0.82 V vs RHE and a peak power density of 640 mW cm^{-2} in 1.0 bar H_2/O_2 fuel cell, which undoubtedly reflects its tendency towards $4e^-$ ORR. It was not until recent years researchers have found that CoN_4 SACs also exhibit high performance in the synthesis of hydrogen peroxide (Sun et al., 2019). This contradictory reminds us that more theoretical and experimental efforts should be made on revealing the underlying electronic structure which causes this activity shift. It also alerts us that activity and selectivity of $2e^-$ ORR could be promoted by carefully tuning the electronic structure of SACs.

In the traditional none-noble metal SACs synthesis, various modulation methods have been developed (Choi et al., 2020; Fan et al., 2020; Wang et al., 2022a; Li et al., 2020b). In general, SACs are usually fixed on a substrate with a central metal atom and coordination atoms (N, O, S, P, etc.). Tuning these coordination atoms (first sphere coordination environment) could be realized by *in situ* heteroatom doping during the

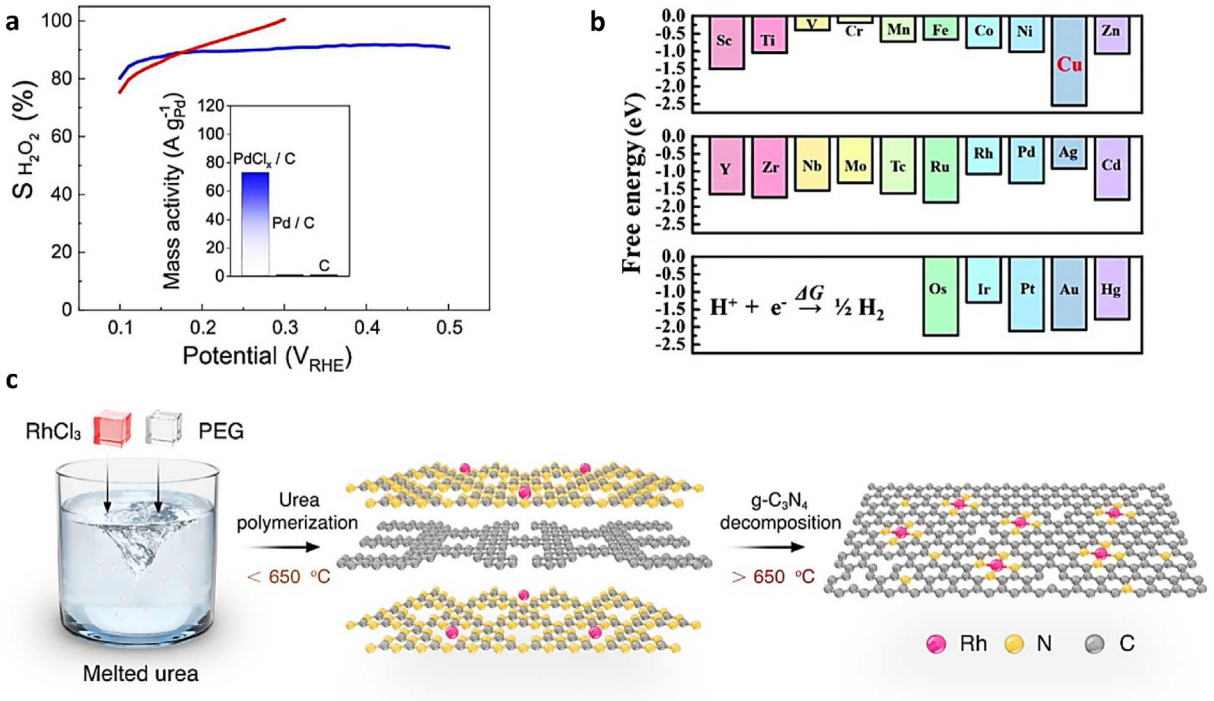

Fig. 3. (a) RRDE results of potential-dependent selectivities S_{H2O2} for $PdCl_x$/C, Pd nanoparticles/C and C (Ledendecker et al., 2020). (b) Calculation of adsorption energy of O_2 molecule on various SACs supported by g-C_3N_4 for side-on and end-on configurations (Cao et al., 2020). (c) Schematic of the synthesis process of enzyme-like Rh_1/NC (Chen et al., 2022c).

synthesis of these SACs. Tailoring second and higher coordination shell could be adopted by introducing functional group or heteroatom doping onto the substrate, or simply changing another substrate with special properties. These adjustment aims to selectively changing the electronic or geometric structure of SACs, and further changing the absorption energy of reaction intermediate (Ramaswamy et al., 2013; Mun et al., 2019). Rate-determining steps and reaction pathways might be changed thus receiving the desired results. In the field of H_2O_2 electro-synthesis, researchers have gained attention to modulate the structure of SACs to enhance activity and selectivity. As a result, a review on the modulating method and the obtained catalytic activity in this field is important.

3.1. Tuning the metal center

Towards the selection of different metal centers, Sun and colleagues scan through a number of transition metal SACs, including Mn, Fe, Co, Ni, Cu (Sun et al., 2019; Luo et al., 2022). Through a comprehensive DFT calculation and using OH* binding free energy (G_{OH*}) as a descriptor. Typically, in order to obtain a high 2e- ORR activity and low overpotential, the OH* binding energy has to be optimized around 1.0 eV and the OOH* binding energy has to be around 4.2 eV, given the scaling relationship between these two intermediates is $G_{*OOH} = G_{*OH} + 3.2$ eV ± 0.2 eV. Through the calculation, they conclude that Co–N–C accommodate on the top of the volcano-like curve (Fig. 4(a)), this moderate binding energy facilitates both the formation and desorption of OOH* intermediates, thus making a compromise between activity and selectivity. Co–N–C exhibits a selectivity of over 80% and a 4 mol peroxide $g_{cat}^{-1}\,h^{-1}$ in a micro-flow cell. This result is verified in Gao's work (Fig. 4(b)) (Gao et al., 2020). They claimed that with the increase in the number of valence electrons in M, the d band of M shift down in energy compared with Fermi level from Mn to Cu, thus the binding energy of OOH* tends to become weaker and Co SAC possesses the most suitable adsorption energy (Fig. 4(c)). A high faraday efficiency of over 90% and a current density of 1 mA cm^{-2} at 0.6 V vs RHE was achieved.

These work plays a critical role in understanding the intrinsic catalytic activity of this type of catalyst. However, there are still some ambiguous parts in the understanding of M-N-C atomic structure, which hinders the precise structure control on a synthesis basis. As a result, six transitional metal covalent organic framework SACs were synthesized and tested (Gao et al., 2020). A pH independent activity trend was revealed, with COF-366-Co being the most active catalyst (Fig. 4(d)), which strongly proved Co SACs as the most promising catalyst towards 2e$^-$ ORR. They also demonstrate the binding energy difference between $*O_2$ and *HOOH (E_{O2*}-E_{HOOH*}) as a new reliable descriptor of 2e$^-$ activity (Fig. 4(e)).

3.2. Tuning the first sphere coordination

In a MN_4 configuration, only CoN_4 shows a promising activity. However, by tuning the first sphere coordination with heteroatoms (O, Cl, P, S, etc.), a selectivity transformation might be shown for other transitional metals (Fe, Ni, Mo, etc.). Jiang and coworkers introduced single-atom sites into oxygen-contained carbon nanotube, and tested their activity in alkaline and neutral electrolyte, with Fe-CNT and Pd-CNT surpassing other comparative samples (Jiang et al., 2019). Fe–C–O motifs unprecedentedly shows a high activity towards 2 e$^-$ ORR, in a sharp contrast with Fe–C–N counterparts. They pointed out that given the plentiful combinations between metal centers and non-metal dopants, the pool of catalytic sites could be successfully enriched, thus providing us with more opportunities to improve activity and control the reaction. Inspired by this idea, several Ni SACs is gaining more attention. A NiN_2O_2 catalyst was designed by Wang and co-workers by a Schiff base ligand-mediated pyrolysis strategy, and 5.9 mol $g_{cat}^{-1}\,h^{-1}$ was achieved at a current density of 70 mA cm^{-2} in 0.1 M KOH (Wang et al., 2020). To take a step forward, a N_4–Ni_1–O_2 catalyst was developed recently, with a single-atom Ni site coordinate with four nitrogen atoms and two oxygen atoms (Fig. 5(a)) (Xiao et al., 2022). By providing this extra O coordination, a remarkable high selectivity of 96% at industrial relevant current 200 mA cm^{-2} was obtained in 1 M KOH, far surpassing other results in alkaline media up to date. Except for the most studied third-period transition metals, a high loading 10 wt% Mo SACs is prone to 2 e$^-$ ORR by O and S atom coordination (Fig. 5(b)), DFT calculations reveal that Mo–S_4–C and Mo–O_3S–C motifs are responsible for 2e$^-$ activity (Fig. 5(c)) (Tang et al., 2020).

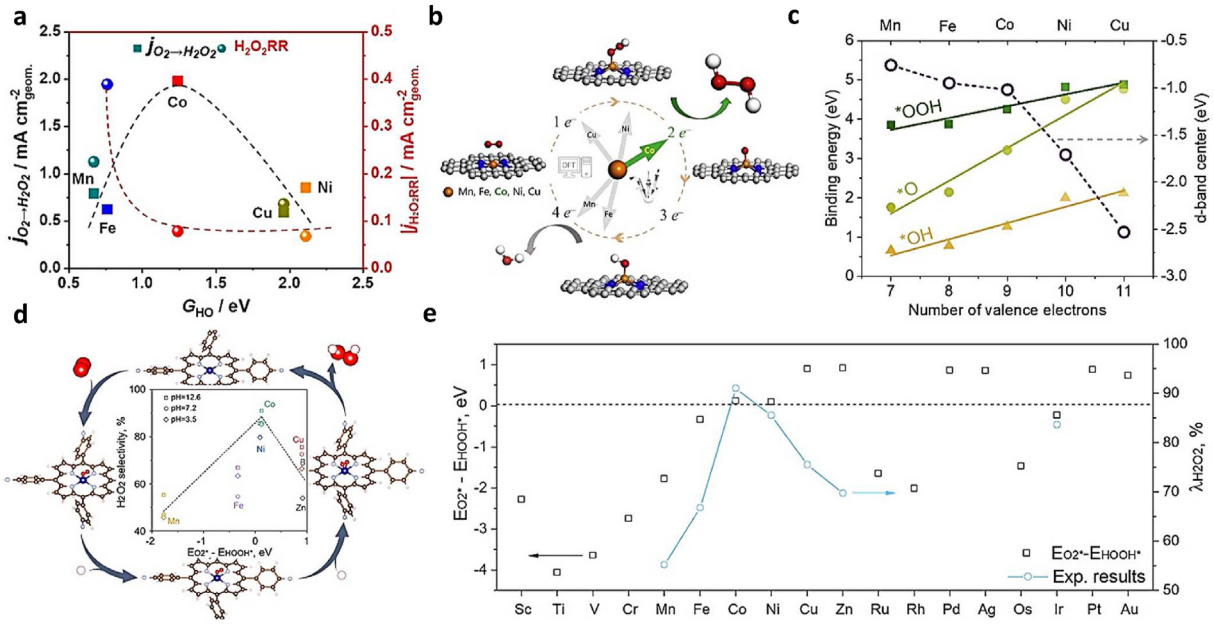

Fig. 4. (a) Thermodynamic activity trend for two electron ORR (black line) and corresponding H_2O_2RR (red line) as a function of *OH binding energy (Xie et al., 2020). (b) Schematic illustration of different 2e$^-$ and 4e$^-$reaction pathways of transitional metal SACs (M = Mn, Fe, Co, Ni, Cu) anchored on N-doped graphene. (c) Binding energy of reaction intermediates (*O, *OH, *OOH) of these transitional metal SACs and the d-band center of metal atoms (Luo et al., 2022). (d) A pH-universal selectivity trend of transitional metal covalent organic framework SACs as a function of descriptor E_{O2}*-E_{HOOH}* and (e) comparison of E_{O2}*-E_{HOOH}* and experimental-measured λ_{H2O2} (H_2O_2 efficiency) (Gao et al., 2020).

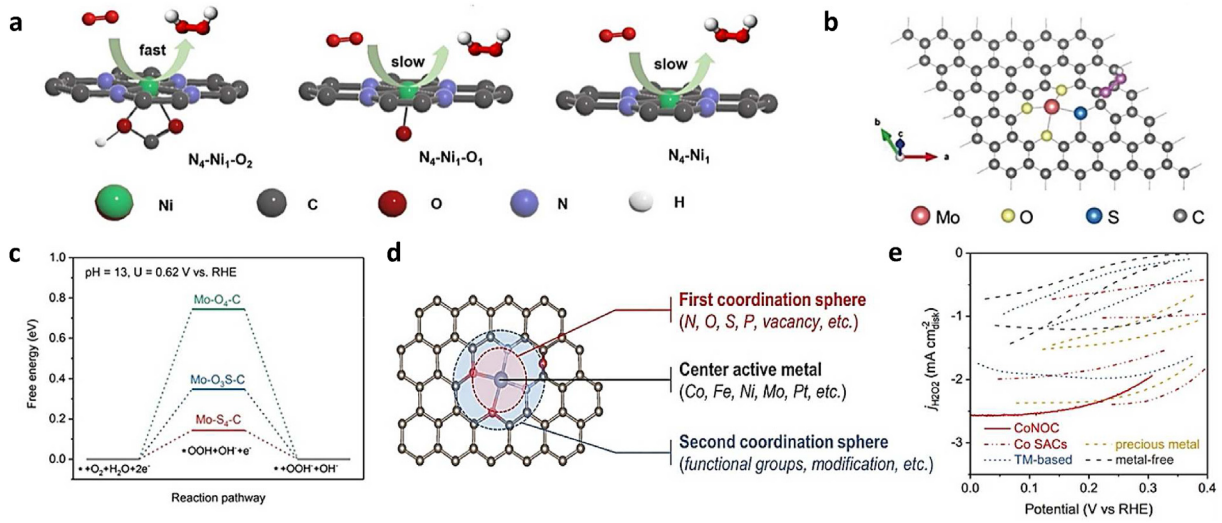

Fig. 5. (a) Plausible reaction pathways of two electron ORR on N_4–Ni_1–O_2, N_4–Ni_1–O_1, N_4–Ni_1 catalysts (Xiao et al., 2022). (b) A schematic illustration of one possible coordination environment of Mo SACs and (c) free energy diagram of three as synthesized Mo SACs structure at the equilibrium potential of the reaction (Tang et al., 2020). (d) Illustration of different modification directions (center atoms, first and second sphere coordination) of SACs and (e) comparison of partial H_2O_2 current densities of CoNOC and other $2e^-$ catalysts in literature (Tang et al., 2021).

As we have discussed above, H_2O_2 decomposition in alkaline electrolyte is very frustrating, which remains an obstacle for real-world usage. For SACs working in acid electrolyte, very recently, Tang and colleagues developed a CoNOC catalyst, EXAFS curve fitting confirm a Co–N_2O_2–C moiety in the first shell coordination (Fig. 5(d)) (Tang et al., 2021). They also claimed the coexistence of epoxy groups in the second shell by examining the Soft XANES O–K edge spectra, these combined give a high H_2O_2 partial current density (Fig. 5(e)) and a productivity of 590 mmol g_{cat}^{-1} h^{-1}. In situ ATR-SEIRAS spectra followed by a DFT calculation supported the idea that the actual activity site shift from the Co-atom center to O adjacent C atoms.

While these studies are critical in understanding SACs in an atomic level, we must keep in mind that the specific coordination environment in the first sphere is still uncertain. Characterization with higher precision for this type of catalyst is still urgently needed. In contrast, tuning the second sphere by involving functional groups or alter the substrate property might be a straighter forward way.

3.3. *Tuning the second and higher sphere coordination*

Introducing oxygen-containing group is one of the most applied strategies in carbon-based materials, Kim and coworkers focus on the

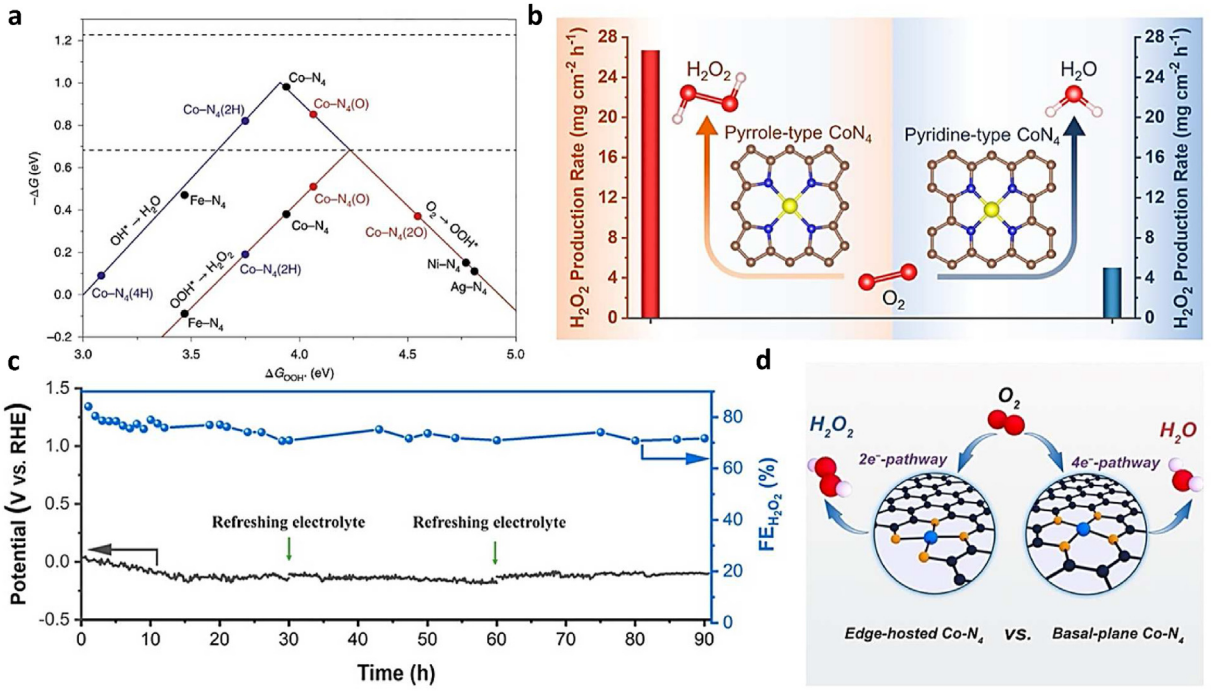

Fig. 6. (a) Calculated volcano-type plot of $4e^-$ and $2e^-$ ORR process, with blue and red dots corresponding to 4H*/2H* and O*/2O* absorbed near the CoN_4/graphene sites (Jung et al., 2020). (b) A graphic illustration of different reaction routes of pyridine-type and pyrrole-type CoN_4 motifs and (c) A 90-h flow-cell electrolysis for Co–N SAC_{DP} in 0.1 M $HClO_4$ at a current density of 50 mA cm^{-2} (Chen et al., 2022b). (d) Structure-function relationship of edge-hosted Co–N_4 and basal-plane Co–N_4 which declares their different $2e^-$ and $4e^-$ properties (Tian et al., 2022).

relationship between oxygen content and activity of carbon nanotubes, and find a positive correlation, which indicates the important role of oxygen-containing groups for hydrogen peroxide activity (Lu et al., 2018). Another work analyzed the types of oxygen-containing groups in oxidized graphene through FTIR spectra and high-resolution oxygen K-edge NEXAFS spectra, and concluded that the ether defects along sheet edges is the most active site (Kim et al., 2018). These studies provide theoretical guidance for the development of metal-free carbon materials under alkaline conditions and promote the development of this class of materials (Guo et al., 2022).

Interestingly, the catalytic properties of CoN_4 could also be enhanced by introducing surrounded oxygen functional groups (Wang et al., 2016). G_{OOH^*} increased from 3.9 eV to 4.1 eV when an O* is absorbed next to CoN_4 moiety, leading to an inclination to the peak value of the volcano-type curve. A similar trend was viewed when two O* groups or an OH* group is absorbed (Fig. 6(a)). This fine-tuning method of the catalytic activity coincide with another work, where spectroscopic and activity results pointed out that the high activity of EA-CoN@CNTs and HE-CoN@CNT originated from the epoxy-groups adjacent CoN_4 sites (Tang et al., 2021).

Aside from oxygen-containing groups, ratio of pyridine-type to pyrrole-type N also greatly influenced the 2 e^- activity according to Chen's work (Chen et al., 2022b). Through a series of experimental results including XPS, EXAFS, O_2-TPD, and in-situ ATR-SEIRAS spectra, they conclude that pyrrole-type CoN_4 is responsible for the $2e^-$ activity, while in sharp contrast pyridine-type N is selective towards $4e^-$ ORR (Fig. 6(b)). In line with the experimental results, a DFT calculation shows a HOO* binding energy of 4.28 for pyrrole-type CoN_4, which is very close to the optimal adsorption energy of 4.22 eV. An admirable value of 2032 mg H_2O_2 production in a 90 h flow-cell electrolysis with a current density of 50 mA cm^{-2} highlighted its potential in real-world electrolysis (Fig. 6(c)).

Most work recently emphasize on tailoring the coordination environment of SACs, however, the geometric state of these sites either at defective pockets or edges of the carbon plane and their corresponding properties are quite ignored in the past. In recent times, Tian and colleagues successfully prepared Co SACs on hierarchically porous carbon (Co–N/HPC) and graphene flakes (Co–N/GFs) (Tian et al., 2022). The edge-rich Co–N/HPC catalyst achieved a high faraday efficiency of over 90%, exceeding the basal plane host sites in Co–N/GFs (Fig. 6(d)). This work indicates that we could tune the SACs activity of $2e^-$ ORR by simply modulate the macroscopic substrate properties and higher shell environment of single-atom sites, which opens up a new orientation for SACs design.

4. SACs working at high current densities

The development of SACs operating at high current densities is closely related with advances in reactor configuration design. The rotating ring-disk electrode (RRDE) is the most commonly used device for testing catalytic activity and selectivity (Chang et al., 2020; Li et al., 2019b). Hydrogen peroxide is generated on the middle catalytic layer and can be simultaneously collected and oxidized by the outer platinum ring for productivity testing. The advantage of this setup is that it allows for a fast screening of well-performing catalysts, however, the activity results obtained are very sensitive to the preparation method of catalyst layer and the amount of catalyst loading. In addition, since the rapid removal of H_2O_2 from the catalytic layer avoids its further reduction to H_2O, testing with this method usually reveals the upper limit of catalyst activity and does not fully reflects the catalytic performance at high current densities (Schmidt et al., 2019; Zhou et al., 2016; Xia et al., 2020). H-type cell is another widely studied electrolytic cell for bulk electrolysis of hydrogen peroxide (Jiang et al., 2019; Guo et al., 2022; Albertin et al., 2022). However, due to its poor stability and unreliable mass transportation, H-type electrolytic cells can barely operate stably for long periods at current densities over 20 mA cm^{-2}. Therefore, in order to further increase the current densities and test the catalysts in harsh conditions, researchers are encouraged to performed their reactions through a gas diffusion electrode (GDE), which has the merits of high mass transfer and continuous acquisition of reaction products (Xia et al., 2021; Wang et al., 2022b; Cao et al., 2021; Chen et al., 2021b; Li et al., 2020c). A natural air gas diffusion electrode was utilized by Zhang and coworkers to test an In SAs/NSBC catalyst with N, S first sphere coordination and B second sphere coordination (Fig. 7(a)) (Zhang et al., 2022a). The production rate was 6.49 mol H_2O_2 g_{catal}^{-1} h^{-1} in alkaline electrolyte and 6.71 mol H_2O_2 g_{catal}^{-1} h^{-1} in neutral electrolyte at a high current density of 90 mA cm^{-2} (Fig. 7(b)). This result undoubtedly exhibits the superior intrinsic activity of this heteroatom-modified In SAC and the excellent performance of this type of reactor.

Aside from the traditional GDE configuration, recent studies also focus on the utilization of membrane electrode assembly (MEA) and porous solid-state electrolyte on H_2O_2 production (Lee et al., 2023). Xia and colleagues first develop a new reactor configuration in which HO_2^- generated at the cathode and H^+ generated at the anode were recombined to form H_2O_2 in the solid-state electrolyte (Fig. 7(c)) (Xia et al., 2019). The remarkable part is that this application of double membrane and solid-state electrolyte successfully resolve the frustrating flooding issue and could obtain a pure H_2O_2 solution without electrolyte ions. Through carefully tuning the E_{cell} and deionized water flow rate, a considerable H_2O_2 partial current of 123 mA cm^{-2} could be reached at cell voltage of 2.71 V, and a tunable H_2O_2 concentration up to 20 wt% could be attained. For single-atom catalysts, a recent work constructed an octafluoro-substituted molecular Co–N–C catalyst, and assessed its H_2O_2 production performance in a flow cell equipped with solid-state electrolyte (Liu et al., 2023b). A maximum H_2O_2 productivity of 10.76 mol H_2O_2 g_{cat}^{-1} h^{-1} at 288 mA cm^{-2} was achieved in this electrolyzer (Fig. 7(d)), and a continuous 9300 ppm H_2O_2 solution could be produced at a DI water flow rate of 12 ml h^{-1} (Fig. 7(e)). Although the inspiring result demonstrates the promising application of SACs in real-world electrolysis, we must notice that the voltage variation will increase at high current densities (E_{cell} increment was 17.1% at 100 mA cm^{-2} etc.). As a result, more efforts are needed to develop SACs working at harsh working conditions and at industrial-relevant current densities.

Another very recent work also tends to solve this problem on a molecular basis. They design a Co single-atom catalyst with cobalt phthalocyanine anchored on the surface of oxygen-modified CNTs, which not only prevents the aggregation of the phthalocyanine molecule, but also successfully tunes the electronic structure of the metal center through a strong metal-support interaction (Cao et al., 2023). This fine-tuning method leads to high faradaic efficiency even at 300 mA cm^{-2} and a superior production rate of 11.527 mol H_2O_2 g_{cat}^{-1} h^{-1} (Fig. 7(f)). with outstanding stability (Fig. 7(g)). These works confirm the promising application of molecular catalysts at high current densities and arouses more precise design for this type of catalyst (Lee et al., 2023).

5. Stability issues and future challenges of SACs

Stability is an important consideration that hinders the practical applications of single-atom catalysts and has become a central issue in fuel cell operations. This is also of particular concern in the field of H_2O_2 synthesis, since H_2O_2 has a strong oxidation capacity and may generate ·OH radicals when encountering single-atom sites (especially iron sites). This could lead to problems such as demetallation and carbon corrosion and may result in a drastic decrease in catalyst activity and selectivity. Nowadays, researcher have dedicated to promote the durability of single-atom catalysts on a synthetic basis.

Demetallation could be relieved by regulating the coordination structure of metal center, or constructing a dual-atomic metal center. Luo and colleagues developed a highly coordinated FeN_4 site (without low coordinated FeN_2/N_3 structure) with both acrylic acid and maleic acid in a copolymer as the precursor (Shao et al., 2019). This coordination structure has an ultra-high binding energy and thus could be sustained in

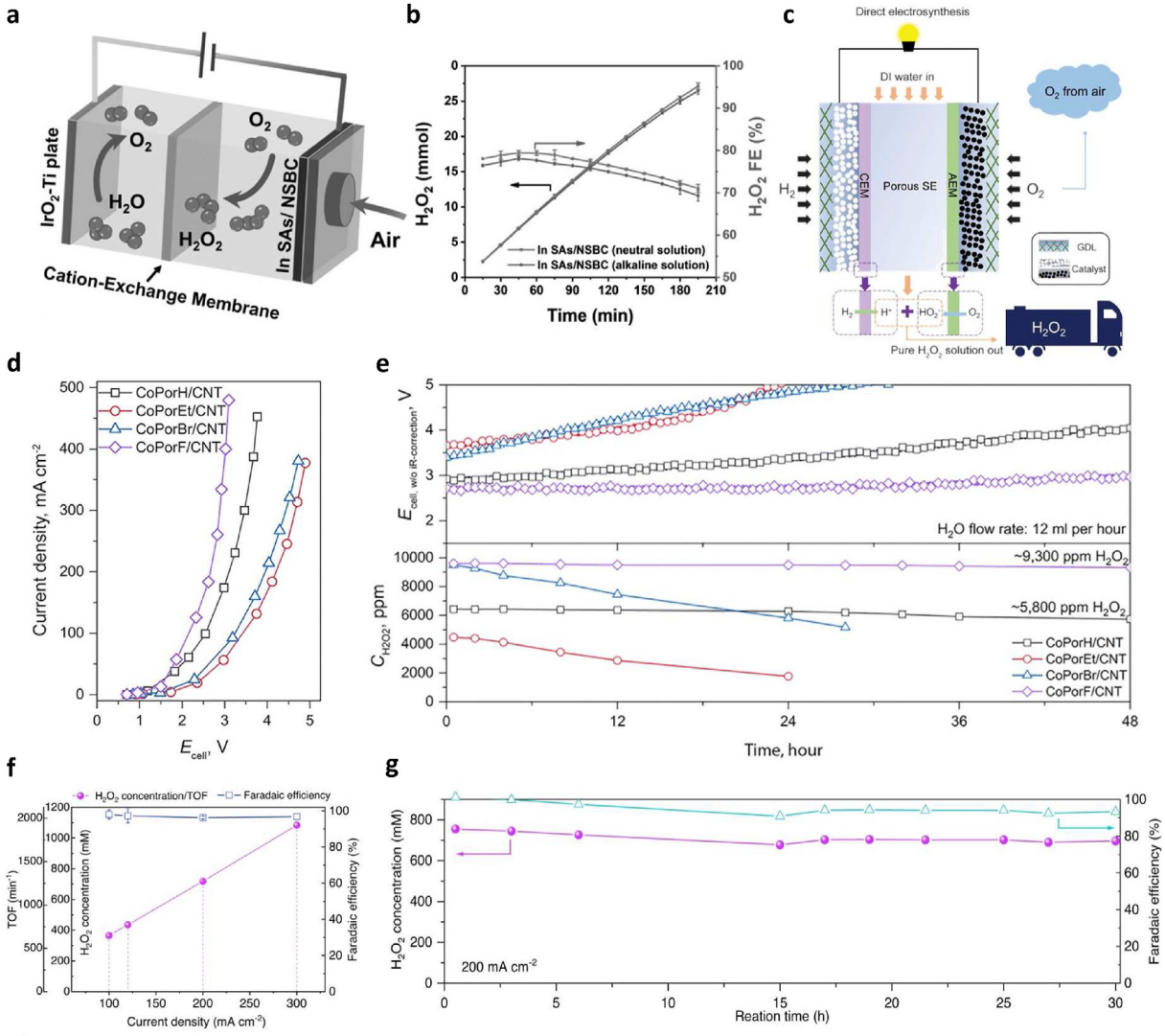

Fig. 7. (a) A schematic illustration of a natural air diffusion electrode using In SAs/NSBC as cathode catalyst, and (b) variation of H_2O_2 production amount and Faraday efficiency with time at a current density of 90 mA cm^{-2} (Zhang et al., 2022a). (c) Electrolysis with a solid-state electrolyte cell with pure H_2 and O_2 as reactants, DI water flows into the solid-state electrolyte and pure H_2O_2 solution was driven out (Xia et al., 2019). (d) Response in current density with increasing cell voltage of the electrolyzer with 80% *iR*-correction and (e) cell voltage change and H_2O_2 concentration for different catalysts during stability test at 50 mA cm^{-2} and a H_2O flow rate of 12 ml h^{-1} (Liu et al., 2023b). (f) H_2O_2 concentration, Faradaic efficiency and TOF values of CoPc-OCNT at industrial-relevant current densities up to 300 mA cm^{-2} (g) Stability evaluation of CoPc-OCNT cathode for continuous electrosynthesis of H_2O_2 at 200 mA cm^{-2} in a chronopotentiometry test (Cao et al., 2023).

a H_2-air fuel cell operation. Another recent work by Chi and coworkers doped Zr in a Fe–N–C catalyst (Chi et al., 2023), and the possible Fe/Zr dual-metal active sites retained 40% of its initial performance in 100 h, far surpassing the original Fe–N–C catalyst. Demetallation is extremely severe when applying a Fe-based catalyst due to the derived free radicals (Xie et al., 2022). Fortunately, Co and Ni based catalysts are promising candidates for the $2e^-$ ORR process and could improve the site stability to some extent.

Carbon corrosion problems are commonly resolved by utilizing highly graphitized carbon substrates or by modifying the structure of carbon substrates. Selecting substrates such as highly graphitized and robust multi-walled carbon nanotubes (MWCNTs) can effectively improve stability. Enhancing the graphitization of the carrier can also be achieved by pyrolysis at ultra-high temperatures (>1100°C). Studies revealed that elevating the temperature to 1200°C can regulate the ratio between unstable D1 sites (O–FeN_4C_{12}) and stable D2 sites (FeN_4C_{10}), thus showing optimized stability (Xia et al., 2023). Liu and colleagues deposited a thin layer of nitrogen-doped carbon onto the atomically dispersed Fe–N–C catalyst and simultaneous transforming defect-rich pyrrolic N sites into highly durable pyridine coordinated sites (Liu et al., 2022). This modified catalyst could even approach the stability performance of a commercial Pt/C catalyst in a membrane electrode assembly. Although the stability of catalysts in fuel cells has been well reported and standardized test protocols have developed, the operational stability in H_2O_2 electrosynthesis (especially with the presence of high concentration H_2O_2 product), has not received much attention and requires more research efforts.

Another future challenge of SACs aside from stability is the ability of scale-up synthesis. A variety of synthetic strategies, including physical and chemical methods, has evolved in recent years for obtaining SACs. However, these methods are often cumbersome and costly. Physical methods, such as atomic layer deposition, suffer from low productivity and high cost, which are not conducive to large-scale production. Chemical methods require tedious synthesis processes. These processes include chemisorption and homogeneous mixing of metal precursors followed by pyrolysis and stabilization as single-atom catalysts on defective and heteroatom-rich carriers. Furthermore, the aggregation of small nanoparticles and single atoms on the support is inevitable, which greatly hinders the scaling up of SACs synthesis. Therefore, it is important to develop inexpensive methods for the synthesis of single-atom catalysts that can be practical applied. Qu

and coworkers developed a simple synthesis strategy to acquire M-SAs/N–C (M = Cu, Co or Ni) from bulk metal foam, which is scalable and feasible for industrial synthesis (Qu et al., 2018). In a word, an affordable synthesize strategy should use inexpensive and readily available metal precursors, nitrogen sources, and carbon substrates, and perform high volume synthesis in as few steps as possible.

6. Conclusion

Electrochemical hydrogen peroxide production through two electron ORR is a green and reliable method for decentralized H_2O_2 production and could be widely used in water treatment, disinfection and chemical synthesis. However, the lack of catalysts understanding and insufficient reactor design strongly impede further development. Nowadays, progress of SACs design brings new anticipation to this field (Lin et al., 2023; Shin et al., 2023).

For the rational design of SACs, the state-of-the-art catalysts should be working at industrial-relevant current densities (e.g. over 200 mA/cm^2), with an acceptable selectivity and long-term stability. However, there are no known materials that meet all of these standards. For the activity and selectivity part, metal-free carbon material catalysts have been extensively studied, and have relatively high activity and selectivity under alkaline conditions. However, due to the inevitable decomposition of H_2O_2 in alkaline electrolyte, the application prospect of metal-centered SACs under acid conditions is promising. Rational design of SACs through modification of metal center, tuning first sphere and second sphere coordination, modulating macroscopic support materials is necessary to overcome the obstacles regarding the balance between ORR activity and H_2O_2 selectivity. DFT calculations and machine learning algorithm should also be involved in predicting and understanding active sites and reaction mechanisms.

For the stability issue of SACs, the demetallation and carbon corrosion problems (Xie et al., 2022; Liu et al., 2022) commonly found in fuel cell MN_4 catalysts will be exacerbated in the presence of hydrogen peroxide, so additional designs are needed to stabilize this class of materials in the future. Previously reported measures (Miao et al., 2022; Du et al., 2021; Li et al., 2018) includes: (1) Designing more stable active sites. (2) Utilizing a highly graphitized carbon substrate. (3) Introducing radical scavenger, and (4) adjusting the structure of the catalyst layer by defect engineering and pore engineering. These efforts will be highly appreciated to enhance the stability of SACs and enable long-term operations, especially in acid electrolyte where active radicals are formed by fenton process. This also reminds us that catalyst materials should be tested at high working densities in gas diffusion electrode or membrane electrode assembly to ensure their use in practical scale production (Xia et al., 2019; Zhang et al., 2022b).

In a word, opportunities and obstacles of SACs still exist in the field of H_2O_2 electro-synthesis. Laboratorial and industrial efforts should be taken to predict catalyst activity, identify active sites and intermediates, develop SACs with high stability and selectivity, and finally put them into commercial use.

Author contributions

H.H. and M.S. contributed equally.

Declaration of competing interest

The authors declare that they have no known competing financial interests or personal relationships that could have appeared to influence the work reported in this paper.

Acknowledgement

This work was supported by the China Postdoctoral Science Foundation (2021M691754).

References

Albertin, S., Merte, L.R., Lundgren, E., Martin, R., Weaver, J.F., Dippel, A.-C., Gutowski, O., Hejral, U., 2022. Oxidation and reduction of Ir(100) studied by high-energy surface X-ray diffraction. J. Phys. Chem. C 126, 5244–5255.

Ayers, K.E., Dalton, L.T., Anderson, E.B., 2012. Efficient generation of high energy density fuel from water. ECS Trans. 41, 27–38.

Barazesh, J.M., Hennebel, T., Jasper, J.T., Sedlak, D.L., 2015. Modular advanced oxidation process enabled by cathodic hydrogen peroxide production. Environ. Sci. Technol. 49, 7391–7399.

Brillas, E., Sires, I., Oturan, M.A., 2009. Electro-fenton process and related electrochemical technologies based on fenton's reaction chemistry. Chem. Rev. 109, 6570–6631.

Brillas, E., Bastida, R.M., Llosa, E., Casado, J., 2019. Electrochemical destruction of aniline and 4-chloroaniline for wastewater treatment using a carbon-PTFE O_2-fed cathode. J. Electrochem. Soc. 142, 1733–1741.

Campos-Martin, J.M., Blanco-Brieva, G., Fierro, J.L.G., 2006. Hydrogen peroxide synthesis: an outlook beyond the anthraquinone process. Angew. Chem. Int. Ed. 45, 6962–6984.

Cao, Y.Y., Zhao, C.X., Fang, Q.J., Zhong, X., Zhuang, G.L., Deng, S.W., Wei, Z.Z., Yao, Z.H., Wang, J.G., 2020. Hydrogen peroxide electrochemical synthesis on hybrid double-atom (Pd-Cu) doped N vacancy g-C_3N_4: a novel design strategy for electrocatalyst screening. J. Mater. Chem. A 8, 2672–2683.

Cao, P., Quan, X., Zhao, K., Zhao, X., Chen, S., Yu, H., 2021. Durable and selective electrochemical H_2O_2 synthesis under a large current enabled by the cathode with highly hydrophobic three-phase architecture. ACS Catal. 11, 13797–13808.

Cao, P., Quan, X., Nie, X., Zhao, K., Liu, Y., Chen, S., Yu, H., Chen, J.G., 2023. Metal single-site catalyst design for electrocatalytic production of hydrogen peroxide at industrial-relevant currents. Nat. Commun. 14, 172.

Caruso, A.A., Del Prete, A., Lazzarino, A.I., Capaldi, R., Grumetto, L., 2020. Might hydrogen peroxide reduce the hospitalization rate and complications of SARS-CoV-2 infection? Infect. Control Hosp. Epidemiol. 41, 1360–1361.

Chang, Q., Zhang, P., Mostaghimi, A.H.B., Zhao, X., Denny, S.R., Lee, J.H., Gao, H., Zhang, Y., Xin, H.L., Siahrostami, S., Chen, J.G., Chen, Z., 2020. Promoting H_2O_2 production via 2-electron oxygen reduction by coordinating partially oxidized Pd with defect carbon. Nat. Commun. 11, 2178.

Chen, B., Wang, T., Zhao, S., Tan, J., Zhao, N., Jiang, S.P., Zhang, Q., Zhou, G., Cheng, H.M., 2021a. Efficient reversible conversion between MoS_2 and Mo/Na_2S enabled by graphene-supported single atom catalysts. Adv. Mater. 33, e2007090.

Chen, S., Luo, T., Chen, K., Lin, Y., Fu, J., Liu, K., Cai, C., Wang, Q., Li, H., Li, X., Hu, J., Li, H., Zhu, M., Liu, M., 2021b. Chemical identification of catalytically active sites on oxygen-doped carbon nanosheet to decipher the high activity for electro-synthesis hydrogen peroxide. Angew. Chem. Int. Ed. 60, 16607–16614.

Chen, B., Zhong, X., Zhou, G., Zhao, N., Cheng, H.M., 2022a. Graphene-supported atomically dispersed metals as bifunctional catalysts for next-generation batteries based on conversion reactions. Adv. Mater. 34, e2105812.

Chen, S., Luo, T., Li, X., Chen, K., Fu, J., Liu, K., Cai, C., Wang, Q., Li, H., Chen, Y., Ma, C., Zhu, L., Lu, Y.R., Chan, T.S., Zhu, M., Cortes, E., Liu, M., 2022b. Identification of the highly active Co-N_4 coordination motif for selective oxygen reduction to hydrogen peroxide. J. Am. Chem. Soc. 144, 14505–14516.

Chen, J., Ma, Q., Zheng, X., Fang, Y., Wang, J., Dong, S., 2022c. Kinetically restrained oxygen reduction to hydrogen peroxide with nearly 100% selectivity. Nat. Commun. 13, 2808.

Chi, B., Zhang, L., Yang, X., Zeng, Y., Deng, Y., Liu, M., Huo, J., Li, C., Zhang, X., Shi, X., Shao, Y., Gu, L., Zheng, L., Cui, Z., Liao, S., Wu, G., 2023. Promoting ZIF-8-derived Fe–N–C oxygen reduction catalysts via Zr doping in proton exchange membrane fuel cells: durability and activity enhancements. ACS Catal. 13, 4221–4230.

Chidambara Raj, C.B., Li Quen, H., 2005. Advanced oxidation processes for wastewater treatment: optimization of UV/H_2O_2 process through a statistical technique. Chem. Eng. Sci. 60, 5305–5311.

Choi, C.H., Kwon, H.C., Yook, S., Shin, H., Kim, H., Choi, M., 2014. Hydrogen peroxide synthesis via enhanced two-electron oxygen reduction pathway on carbon-coated Pt surface. J. Phys. Chem. C 118, 30063–30070.

Choi, C.H., Kim, M., Kwon, H.C., Cho, S.J., Yun, S., Kim, H.T., Mayrhofer, K.J., Kim, H., Choi, M., 2016. Tuning selectivity of electrochemical reactions by atomically dispersed platinum catalyst. Nat. Commun. 7, 10922.

Choi, S., Chung, M., Kim, D., Kim, S., Yun, K., Cha, W., Harder, R., Kawaguchi, T., Liu, Y., Ulvestad, A., You, H., Song, M.K., Kim, H., 2020. In situ strain evolution on pt nanoparticles during hydrogen peroxide decomposition. Nano Lett. 20, 8541–8548.

Chung, H.T., Cullen, D.A., Higgins, D., Sneed, B.T., Holby, E.F., More, K.L., Zelenay, P., 2017. Direct atomic-level insight into the active sites of a high-performance PGM-free ORR catalyst. Science 357, 479–484.

Ciriminna, R., Albanese, L., Meneguzzo, F., Pagliaro, M., 2016. Hydrogen peroxide: a key chemical for today's sustainable development. ChemSusChem 9, 3374–3381.

Cui, X., Li, W., Ryabchuk, P., Junge, K., Beller, M., 2018. Bridging homogeneous and heterogeneous catalysis by heterogeneous single-metal-site catalysts. Nat. Catal. 1, 385–397.

Du, L., Prabhakaran, V., Xie, X., Park, S., Wang, Y., Shao, Y., 2021. Low-PGM and PGM-free catalysts for proton exchange membrane fuel cells: stability challenges and material solutions. Adv. Mater. 33, e1908232.

Fan, M., Cui, J., Wu, J., Vajtai, R., Sun, D., Ajayan, P.M., 2020. Improving the catalytic activity of carbon-supported single atom catalysts by polynary metal or heteroatom doping. Small 16, e1906782.

Flores, M.J., Brandi, R.J., Cassano, A.E., Labas, M.D., 2012. Chemical disinfection with H_2O_2 – the proposal of a reaction kinetic model. Chem. Eng. J. 198–199, 388–396.
Fuku, K., Miyase, Y., Miseki, Y., Gunji, T., Sayama, K., 2017. $WO_3/BiVO_4$ photoanode coated with mesoporous Al_2O_3 layer for oxidative production of hydrogen peroxide from water with high selectivity. RSC Adv. 7, 47619–47623.
Gao, J., Liu, B., 2020. Progress of electrochemical hydrogen peroxide synthesis over single atom catalysts. ACS Mater. Lett. 2, 1008–1024.
Gao, J., Yang, H.b., Huang, X., Hung, S.-F., Cai, W., Jia, C., Miao, S., Chen, H.M., Yang, X., Huang, Y., Zhang, T., Liu, B., 2020. Enabling direct h_2o_2 production in acidic media through rational design of transition metal single atom catalyst. Chem 6, 658–674.
Gong, S., Sun, M., Lee, Y., Becknell, N., Zhang, J., Wang, Z., Zhang, L., Niu, Z., 2023. Bulk-like Pt(100)-oriented ultrathin surface: combining the merits of single crystals and nanoparticles to boost oxygen reduction reaction. Angew. Chem. Int. Ed. 62, e202214516.
Guo, Y., Zhang, R., Zhang, S., Hong, H., Zhao, Y., Huang, Z., Han, C., Li, H., Zhi, C., 2022. Ultrahigh oxygen-doped carbon quantum dots for highly efficient H_2O_2 production via two-electron electrochemical oxygen reduction. Energy Environ. Sci. 15, 4167–4174.
Hage, R., Lienke, A., 2005. Applications of transition-metal catalysts to textile and wood-pulp bleaching. Angew. Chem. Int. Ed. 45, 206–222.
He, Y., Hwang, S., Cullen, D.A., Uddin, M.A., Langhorst, L., Li, B., Karakalos, S., Kropf, A.J., Wegener, E.C., Sokolowski, J., Chen, M., Myers, D., Su, D., More, K.L., Wang, G., Litster, S., Wu, G., 2019. Highly active atomically dispersed CoN_4 fuel cell cathode catalysts derived from surfactant-assisted MOFs: carbon-shell confinement strategy. Energy Environ. Sci. 12, 250–260.
Jatta, M., Kiefer, C., Patolia, H., Pan, J., Harb, C., Marr, L.C., Baffoe-Bonnie, A., 2021. N95 reprocessing by low temperature sterilization with 59% vaporized hydrogen peroxide during the 2020 COVID-19 pandemic. Am. J. Infect. Control 49, 8–14.
Jiang, Y.Y., Ni, P.J., Chen, C.X., Lu, Y.Z., Yang, P., Kong, B., Fisher, A., Wang, X., 2018. Selective electrochemical h_2o_2 production through two-electron oxygen electrochemistry. Adv. Energy Mater. 8.
Jiang, K., Back, S., Akey, A.J., Xia, C., Hu, Y., Liang, W., Schaak, D., Stavitski, E., Norskov, J.K., Siahrostami, S., Wang, H., 2019. Highly selective oxygen reduction to hydrogen peroxide on transition metal single atom coordination. Nat. Commun. 10, 3997.
Jiang, K., Zhao, J., Wang, H., 2020. Catalyst design for electrochemical oxygen reduction toward hydrogen peroxide. Adv. Funct. Mater. 30, 2003321.
Jirkovsky, J.S., Panas, I., Ahlberg, E., Halasa, M., Romani, S., Schiffrin, D.J., 2011. Single atom hot-spots at Au-Pd nanoalloys for electrocatalytic H_2O_2 production. J. Am. Chem. Soc. 133, 19432–19441.
Jung, E., Shin, H., Lee, B.H., Efremov, V., Lee, S., Lee, H.S., Kim, J., Hooch Antink, W., Park, S., Lee, K.S., Cho, S.P., Yoo, J.S., Sung, Y.E., Hyeon, T., 2020. Atomic-level tuning of Co-N-C catalyst for high-performance electrochemical H_2O_2 production. Nat. Mater. 19, 436–442.
Kaiser, S.K., Fako, E., Manzocchi, G., Krumeich, F., Hauert, R., Clark, A.H., Safonova, O.V., Lopez, N., Perez-Ramirez, J., 2020. Nanostructuring unlocks high performance of platinum single-atom catalysts for stable vinyl chloride production. Nat. Catal. 3, 376–385.
Kim, H.W., Ross, M.B., Kornienko, N., Zhang, L., Guo, J., Yang, P., McCloskey, B.D., 2018. Efficient hydrogen peroxide generation using reduced graphene oxide-based oxygen reduction electrocatalysts. Nat. Catal. 1, 282–290.
Kim, H.E., Lee, I.H., Cho, J., Shin, S., Ham, H.C., Kim, J.Y., Lee, H., 2019. Palladium single-atom catalysts supported on $C@C_3N_4$ for electrochemical reactions. Chemelectrochem 6, 4757–4764.
Kim, J.H., Shin, D., Lee, J., Baek, D.S., Shin, T.J., Kim, Y.T., Jeong, H.Y., Kwak, J.H., Kim, H., Joo, S.H., 2020. A general strategy to atomically dispersed precious metal catalysts for unravelling their catalytic trends for oxygen reduction reaction. ACS Nano 14, 1990–2001.
Kodavatiganti, S., Bhat, A.P., Gogate, P.R., 2021. Intensified degradation of Acid Violet 7 dye using ultrasound combined with hydrogen peroxide, Fenton, and persulfate. Sep. Purif. Technol. 279, 119673.
Kosaka, K., Yamada, H., Shishida, K., Echigo, S., Minear, R.A., Tsuno, H., Matsui, S., 2001. Evaluation of the treatment performance of a multistage ozone/hydrogen peroxide process by decomposition by-products. Water Res. 35, 3587–3594.
Kosydar, R., Drelinkiewicz, A., Ganhy, J.P., 2010. Degradation reactions in anthraquinone process of hydrogen peroxide synthesis. Catal. Lett. 139, 105–113.
Lane, B.S., Burgess, K., 2003. Metal-catalyzed epoxidations of alkenes with hydrogen peroxide. Chem. Rev. 103, 2457–2473.
Ledendecker, M., Pizzutilo, E., Malta, G., Fortunato, G.V., Mayrhofer, K.J.J., Hutchings, G.J., Freakley, S.J., 2020. Isolated Pd sites as selective catalysts for electrochemical and direct hydrogen peroxide synthesis. ACS Catal. 10, 5928–5938.
Lee, B.H., Shin, H., Rasouli, A.S., Choubisa, H., Ou, P., Dorakhan, R., Grigioni, I., Lee, G., Shirzadi, E., Miao, R.K., Wicks, J., Park, S., Seok, H., Zhang, J., Chen, Y., Chen, Z., Sinton, D., Hyeno, T., Sung, Y.E., Sargent, E.H., 2023. Supramolecular tuning of supported metal phthalocyanine catalysts for hydrogen peroxide electrosynthesis. Nat. Catal. 6, 234–243.
Li, J., Chen, M., Cullen, D.A., Hwang, S., Wang, M., Li, B., Liu, K., Karakalos, S., Lucero, M., Zhang, H., Lei, C., Xu, H., Sterbinsky, G.E., Feng, Z., Su, D., More, K.L., Wang, G., Wang, Z., Wu, G., 2018. Atomically dispersed manganese catalysts for oxygen reduction in proton-exchange membrane fuel cells. Nat. Catal. 1, 935–945.
Li, J., Jiao, L., Wegener, E., Richard, L.L., Liu, E., Zitolo, A., Sougrati, M.T., Mukerjee, S., Zhao, Z., Huang, Y., Yanf, F., Zhong, S., Xu, H., Krolpf, A.J., Jaouen, F., Myers, D.J., Jia, Q., 2019a. Evolution pathway from iron compounds to Fe1(II)–N_4 sites through gas-phase iron during pyrolysis. J. Am. Chem. Soc. 142, 1417–1423.
Li, B.Q., Zhao, C.X., Liu, J.N., Zhang, Q., 2019b. Electrosynthesis of hydrogen peroxide synergistically catalyzed by atomic Co-N_x-C sites and oxygen functional groups in noble-metal-free electrocatalysts. Adv. Mater. 31, e1808173.
Li, Z., Ji, S., Liu, Y., Cao, X., Tian, S., Chen, Y., Niu, Z., Li, Y., 2020a. Well-defined materials for heterogeneous catalysis: from nanoparticles to isolated single-atom sites. Chem. Rev. 120, 623–682.
Li, X., Rong, H., Zhang, J., Wang, D., Li, Y., 2020b. Modulating the local coordination environment of single-atom catalysts for enhanced catalytic performance. Nano Res. 13, 1842–1855.
Li, L., Tang, C., Zheng, Y., Xia, B., Zhou, X., Xu, H., Qiao, S.Z., 2020c. Tailoring selectivity of electrochemical hydrogen peroxide generation by tunable pyrrolic-nitrogen-carbon. Adv. Energy Mater. 10, 2000789.
Lin, R., Kang, L., Lisowska, K., He, W., Zhao, S., Hayama, S., Hutchings, G.J., Brett, D.J.L., CoràF, F., Parkin, I.P., He, G., 2023. Approaching theoretical performances of electrocatalytic hydrogen peroxide generation by cobalt-nitrogen moieties. Angew. Chem. Int. Ed. 62, e202301433.
Liu, G., Robertson, A.W., Li, M.M., Kuo, W.C.H., Darby, M.T., Muhieddine, M.H., Lin, Y.C., Suenaga, K., Stamatakis, M., Warner, J.H., Tsang, S.C.E., 2017. MoS_2 monolayer catalyst doped with isolated Co atoms for the hydrodeoxygenation reaction. Nat. Chem. 9, 810–816.
Liu, S., Li, C., Zachman, M.J., Zeng, Y., Yu, H., Li, B., Wang, M., Braaten, J., Liu, J., Meyer, H.M., Lucero, M., Kropf, A.J., Alp, E.E., Gong, Q., Shi, Q., Feng, Z., Xu, H., Wang, G., Myers, D.J., Xie, J., Cullen, D.A., Litster, S., Wu, G., 2022. Atomically dispersed iron sites with a nitrogen–carbon coating as highly active and durable oxygen reduction catalysts for fuel cells. Nat. Energy 7, 652–663.
Liu, X.C., Zhang, K.X., Song, J.S., Zhou, G.N., Li, W.Q., Ding, R.R., Wang, J., Zheng, X., Wang, G., Mu, Y., 2023a. Tuning Fe_3O_4 for sustainable cathodic heterogeneous electro-Fenton catalysis by acetylated chitosan. Proc. Natl. Acad. Sci. U.S.A. 120, e2213480120.
Liu, C., Yu, Z., She, F., Chen, J., Liu, F., Qu, J., Cairney, J.M., Wu, C., Liu, K., Yang, W., Zheng, H., Chen, Y., Li, H., Wei, L., 2023b. Heterogeneous molecular Co–N–C catalysts for efficient electrochemical H_2O_2 synthesis. Energy Environ. Sci. 16, 446–459.
Lu, Z., Chen, G., Siahrostami, S., Chen, Z., Liu, K., Xie, J., Liao, L., Wu, T., Lin, D., Liu, Y., Jaramillo, T.F., Nørskov, J.K., Cui, Y., 2018. High-efficiency oxygen reduction to hydrogen peroxide catalysed by oxidized carbon materials. Nat. Catal. 1, 156–162.
Luo, F., Wagner, S., Ju, W., Primbs, M., Li, S., Wang, H., Kramm, U.I., Strasser, P., 2022. Kinetic diagnostics and synthetic design of platinum group metal-free electrocatalysts for the oxygen reduction reaction using reactivity maps and site utilization descriptors. J. Am. Chem. Soc. 144, 13487–13498.
Mun, Y., Lee, S., Kim, K., Kim, S., Lee, S., Han, J.W., Lee, J., 2019. Versatile strategy for tuning ORR activity of a single Fe-N_4 Site by controlling electron-withdrawing/donating properties of a carbon plane. J. Am. Chem. Soc. 141, 6254–6262.
Noyori, R., Aoki, M., Sato, K., 2003. Green oxidation with aqueous hydrogen peroxide. Chem. Commun. 1977–1986.
Perry, S.C., Pangotra, D., Vieira, L., Csepei, L.-I., Sieber, V., Wang, L., Ponce de León, C., Walsh, F.C., 2019. Electrochemical synthesis of hydrogen peroxide from water and oxygen. Nat. Rev. Chem 3, 442–458.
Qiang, Z., Chang, J.H., Huang, C.P., 2002. Electrochemical generation of hydrogen peroxide from dissolved oxygen in acidic solutions. Water Res. 36, 85–94.
Qiao, B., Wang, A., Yang, X., Allard, L.F., Jiang, Z., Cui, Y., Liu, J., Li, J., Zhang, T., 2011. Single-atom catalysis of CO oxidation using Pt_1/FeO_x. Nat. Chem. 3, 634–641.
Qin, R., Liu, K., Wu, Q., Zheng, N., 2020. Surface coordination chemistry of atomically dispersed metal catalysts. Chem. Rev. 120, 11810–11899.
Qu, Y., Li, Z., Chen, W., Lin, Y., Yuan, T., Yang, Z., Zhao, C., Wang, J., Zhao, C., Wang, X., Zhou, F., Wu, Z. Zhuang Y., Li, Y., 2018. Direct transformation of bulk copper into copper single sites via emitting and trapping of atoms. Nat. Catal. 1, 781–786.
Ramaswamy, N., Tylus, U., Jia, Q., Mukerjee, S., 2013. Activity descriptor identification for oxygen reduction on nonprecious electrocatalysts: linking surface science to coordination chemistry. J. Am. Chem. Soc. 135, 15443–15449.
Ro, I., Qi, J., Lee, S., Xu, M., Yan, X., Xie, Z., Zakem, G., Morales, A., Chen, J.G., Pan, X., Vlachos, D.G., Caratzoulas, S., Christopher, P., 2022. Bifunctional hydroformylation on heterogeneous Rh-WO_x pair site catalysts. Nature 609, 287–292.
Santacesaria, E., Di Serio, M., Russo, A., Leone, U., Velotti, R., 1999. Kinetic and catalytic aspects in the hydrogen peroxide production via anthraquinone. Chem. Eng. Sci. 54, 2799–2806.
Santacesaria, E., Di Serio, M., Velotti, R., Leone, U., 2002. Kinetics, mass transfer, and palladium catalyst deactivation in the hydrogenation step of the hydrogen peroxide synthesis via anthraquinone. Ind. Eng. Chem. Res. 33, 277–284.
Schmidt, T.J., Gasteiger, H.A., Stäb, G.D., Urban, P.M., Kolb, D.M., Behm, R.J., 2019. Characterization of high-surface-area electrocatalysts using a rotating disk electrode configuration. J. Electrochem. Soc. 145, 2354–2358.
Shao, Y., Dodelet, J.P., Wu, G., Zelenay, P., 2019. PGM-free cathode catalysts for PEM fuel cells: a mini-review on stability challenges. Adv. Mater. 31, 1807615.
Shen, R., Chen, W., Peng, Q., Lu, S., Zheng, L., Cao, X., Wang, Y., Zhu, W., Zhang, J., Zhuang, Z., Chen, C., Wang, D., Li, Y., 2019. High-concentration single atomic Pt Sites on hollow CuS_x for selective O_2 reduction to H_2O_2 in acid solution. Chem 5, 2099–2110.
Sheng, W., Gasteiger, H.A., Shao-Horn, Y., 2010. Hydrogen oxidation and evolution reaction kinetics on platinum: acid vs alkaline electrolytes. J. Electrochem. Soc. 157, B1529.
Shi, X., Siahrostami, S., Li, G.L., Zhang, Y., Chakthranont, P., Studt, F., Jaramillo, T.F., Zheng, X., Norskov, J.K., 2017. Understanding activity trends in electrochemical water oxidation to form hydrogen peroxide. Nat. Commun. 8, 701.
Shin, H., Lee, S., Sung, Y.E., 2023. Industrial-scale H_2O_2 electrosynthesis in practical electrochemical cell systems. Curr. Opin. Electrochem. 38, 101224.

Siahrostami, S., Verdaguer-Casadevall, A., Karamad, M., Deiana, D., Malacrida, P., Wickman, B., Escudero-Escribano, M., Paoli, E.A., Frydendal, R., Hansen, T.W., Chorkendorff, I., Stephens, I.E., Rossmeisl, J., 2013. Enabling direct H_2O_2 production through rational electrocatalyst design. Nat. Mater. 12, 1137–1143.

Song, X., Li, N., Zhang, H., Wang, L., Yan, Y., Wang, H., Wang, L., Bian, Z., 2020. Graphene-supported single nickel atom catalyst for highly selective and efficient hydrogen peroxide production. ACS Appl. Mater. Interfaces 12, 17519–17527.

Stamenkovic, V.R., Fowler, B., Mun, B.S., Wang, G.F., Ross, P.N., Lucas, C.A., Markovic, N.M., 2007. Improved oxygen reduction activity on $Pt_3Ni(111)$ via increased surface site availability. Science 315, 493–497.

Su, H., Zhou, W., Zhang, H., Zhou, W., Zhao, X., Li, Y., Liu, M., Cheng, W., Liu, Q., 2020. Dynamic evolution of solid-liquid electrochemical interfaces over single-atom active sites. J. Am. Chem. Soc. 142, 12306–12313.

Sun, Y., Silvioli, L., Sahraie, N.R., Ju, W., Li, J., Zitolo, A., Li, S., Bagger, A., Arnarson, L., Wang, X., Moeller, T., Bernsmeier, D., Rossmeisl, J., Jaouen, F., Strasser, P., 2019. Activity-selectivity trends in the electrochemical production of hydrogen peroxide over single-site metal-nitrogen-carbon catalysts. J. Am. Chem. Soc. 141, 12372–12381.

Sun, M., Gong, S., Zhang, Y.-X., Niu, Z., 2022. A perspective on the PGM-free metal–nitrogen–carbon catalysts for PEMFC. J. Energy Chem. 67, 250–254.

Tang, C., Jiao, Y., Shi, B., Liu, J.N., Xie, Z., Chen, X., Zhang, Q., Qiao, S.Z., 2020. Coordination tunes selectivity: two-electron oxygen reduction on high-loading molybdenum single-atom catalysts. Angew. Chem. Int. Ed. 59, 9171–9176.

Tang, C., Chen, L., Li, H., Li, L., Jiao, Y., Zheng, Y., Xu, H., Davey, K., Qiao, S.Z., 2021. Tailoring acidic oxygen reduction selectivity on single-atom catalysts via modification of first and second coordination spheres. J. Am. Chem. Soc. 143, 7819–7827.

Wang, L., Zhang, W., Wang, S., Gao, Z., Luo, Z., Wang, X., Zeng, R., Li, A., Li, H., Wang, M., Zheng, X., Zhu, J., Zhang, W., Ma, C., Si, R., Zeng, J., 2016. Atomic-level insights in optimizing reaction paths for hydroformylation reaction over Rh/CoO single-atom catalyst. Nat. Commun. 7, 14036.

Tian, Y., Li, M., Wu, Z., Sun, Q., Yuan, D., Johannessen, B., Xu, L., Wang, Y., Dou, Y., Zhao, H., Zhang, S., 2022. Edge-hosted atomic Co-N_4 Sites on hierarchical porous carbon for highly selective two-electron oxygen reduction reaction. Angew. Chem. Int. Ed. 61, e202213296.

Wang, X.X., Cullen, D.A., Pan, Y.T., Hwang, S., Wang, M., Feng, Z., Wang, J., Engelhard, M.H., Zhang, H., He, Y., Shao, Y., Su, D., More, K.L., Spendelow, J.S., Wu, G., 2018. Nitrogen-coordinated single cobalt atom catalysts for oxygen reduction in proton exchange membrane fuel cells. Adv. Mater. 30, 1706758.

Wang, Y., Shi, R., Shang, L., Waterhouse, G.I.N., Zhao, J., Zhang, Q., Gu, L., Zhang, T., 2020. High-efficiency oxygen reduction to hydrogen peroxide catalyzed by nickel single-atom catalysts with tetradentate N_2O_2 coordination in a three-phase flow cell. Angew. Chem. Int. Ed. 59, 13057–13062.

Wang, Y., Wang, D., Li, Y., 2022a. Atom-level interfacial synergy of single-atom site catalysts for electrocatalysis. J. Energy Chem. 65, 103–115.

Wang, Y., Shi, R., Shang, L., Peng, L., Chu, D., Han, Z., Waterhouse, G.I.N., Zhang, R., Zhang, T., 2022b. Vertical graphene array for efficient electrocatalytic reduction of oxygen to hydrogen peroxide. Nano Energy 96, 107046.

Xia, C., Xia, Y., Zhu, P., Fan, L., Wang, H., 2019. Direct electrosynthesis of pure aqueous H_2O_2 solutions up to 20% by weight using a solid electrolyte. Science 366, 226–231.

Xia, C., Kim, J.Y., Wang, H., 2020. Recommended practice to report selectivity in electrochemical synthesis of H_2O_2. Nat. Catal. 3, 605–607.

Xia, Y., Zhao, X., Xia, C., Wu, Z.Y., Zhu, P., Kim, J.Y.T., Bai, X., Gao, G., Hu, Y., Zhong, J., Liu, Y., Wang, H., 2021. Highly active and selective oxygen reduction to H_2O_2 on boron-doped carbon for high production rates. Nat. Commun. 12, 4225.

Xia, D., Tang, X., Dai, S., Ge, R., Rykov, A., Wang, J., Huang, T.H., Wang, K.W., Wei, Y., Zhang, K., Li, J., Gan, L., Kang, F., 2023. Ultrastable Fe–N–C fuel cell electrocatalysts by eliminating non-coordinating nitrogen and regulating coordination structures at high temperatures. Adv. Mater. 35, 2204474.

Xie, X., He, C., Li, B., He, Y., Cullen, D.A., Wegener, E.C., Kropf, A.J., Martinez, U., Cheng, Y., Engelhard, M.H., Bowden, M.E., Song, M., Lemmon, T., Li, X.S., Nie, Z., Liu, J., Myers, D.J., Zelenay, P., Wang, G., Wu, G., Ramani, V., Shao, Y., 2020. Performance enhancement and degradation mechanism identification of a single-atom Co–N–C catalyst for proton exchange membrane fuel cells. Nat. Catal. 3, 1044–1054.

Xie, H., Xie, X., Hu, G., Prabhakaran, V., Saha, S., Gonzalez-Lopez, L., Phakatkar, A.H., Hong, M., Wu, M., Shahbazian-Yassar, R., Ramani, V., Al-Sheikhly, M.I., Jiang, D.-e., Shao, Y., Hu, L., 2022. Ta–TiO_x nanoparticles as radical scavengers to improve the durability of Fe–N–C oxygen reduction catalysts. Nat. Energy 7, 281–289.

Xu, J., Zheng, X., Feng, Z., Lu, Z., Zhang, Z., Huang, W., Li, Y., Vuckovic, D., Li, Y., Dai, S., Chen, G., Wang, K., Wang, H., Chen, J.K., Mitch, W., Cui, Y., 2021. Organic wastewater treatment by a single-atom catalyst and electrolytically produced H_2O_2. Nat. Sustain. 4, 233–241.

Yamanaka, I., Murayama, T., 2008. Neutral H_2O_2 synthesis by electrolysis of water and O_2. Angew. Chem. Int. Ed. 47, 1900–1902.

Yang, S., Tak, Y.J., Kim, J., Soon, A., Lee, H., 2017. Support effects in single-atom platinum catalysts for electrochemical oxygen reduction. ACS Catal. 7, 1301–1307.

Yang, S., Verdaguer-Casadevall, A., Arnarson, L., Silvioli, L., Čolić, V., Frydendal, R., Rossmeisl, J., Chorkendorff, I., Stephens, I.E.L., 2018. Toward the decentralized electrochemical production of h_2o_2: a focus on the catalysis. ACS Catal. 8, 4064–4081.

Zhang, J., Zhao, Y., Guo, X., Chen, C., Dong, C.-L., Liu, R.-S., Han, C.-P., Li, Y., Gogotsi, Y., Wang, G., 2018. Single platinum atoms immobilized on an MXene as an efficient catalyst for the hydrogen evolution reaction. Nat. Catal. 1, 985–992.

Zhang, J., Zhang, H., Cheng, M.J., Lu, Q., 2020a. Tailoring the electrochemical production of h_2o_2 : strategies for the rational design of high-performance electrocatalysts. Small 16, e1902845.

Zhang, X., Xia, Y., Xia, C., Wang, H., 2020b. Insights into practical-scale electrochemical H_2O_2 synthesis. Trends Chem 2, 942–953.

Zhang, S., Wu, Y., Zhang, Y.-X., Niu, Z., 2021. Dual-atom catalysts: controllable synthesis and electrocatalytic applications. Sci. China Chem. 64, 1908–1922.

Zhang, E., Tao, L., An, J., Zhang, J., Meng, L., Zheng, X., Wang, Y., Li, N., Du, S., Zhang, J., Wang, D., Li, Y., 2022a. Engineering the local atomic environments of indium single-atom catalysts for efficient electrochemical production of hydrogen peroxide. Angew. Chem. Int. Ed. 61, e202117347.

Zhang, X., Zhao, X., Zhu, P., Adler, Z., Wu, Z.Y., Liu, Y., Wang, H., 2022b. Electrochemical oxygen reduction to hydrogen peroxide at practical rates in strong acidic media. Nat. Commun. 13, 2880.

Zhang, Y.X., Zhang, S., Huang, H., Liu, X., Li, B., Lee, Y., Wang, X., Bai, Y., Sun, M., Wu, Y., Gong, S., Liu, X., Zhuang, Z., Tan, T., Niu, Z., 2023. General synthesis of a diatomic catalyst library via a macrocyclic precursor-mediated approach. J. Am. Chem. Soc. 145, 4819–4827.

Zhao, C.X., Li, B.Q., Liu, J.N., Zhang, Q., 2020. Intrinsic Electrocatalytic activity regulation of M–N–C single-atom catalysts for the oxygen reduction reaction. Angew. Chem. Int. Ed. 60, 4448–4463.

Zhou, R., Zheng, Y., Jaroniec, M., Qiao, S.-Z., 2016. Determination of the electron transfer number for the oxygen reduction reaction: from theory to experiment. ACS Catal. 6, 4720–4728.

Zhou, X., Ke, M.K., Huang, G.X., Chen, C., Chen, W., Liang, K., Qu, Y., Wang, J., Li, F., Yu, H.Q., Wu, Y., 2022. Identification of Fenton-like active Cu sites by heteroatom modulation of electronic density. Proc. Natl. Acad. Sci. U.S.A. 119, e2119492119.

Zhu, Y., Peng, W., Li, Y., Zhang, G., Zhang, F., Fan, X., 2019. Modulating the electronic structure of single-atom catalysts on 2D nanomaterials for enhanced electrocatalytic performance. Small Methods 3, 1800438.

Miao, Z., Li, S., Priest, C., Wang, T., Wu, G., Li, Q., 2022. Effective approaches for designing stable M-N_x/C oxygen-reduction catalysts for proton-exchange-membrane fuel cells. Adv. Mater. 34, e2200595.

Xiao, C., Cheng, L., Zhu, Y., Wang, G., Chen, L., Wang, Y., Chen, R., Li, Y., Li, C., 2022. Super-coordinated nickel N4-Ni1-O2 site single-atom catalyst for selective H_2O_2 electrosynthesis at high current densities. Angew. Chem. Int. Ed. 61, e202206544.